Comparative experiments on a novel CaCl2-based composite material and zeolite 13X inside a sorption reactor for solar heat storage

Elise Bérut, Jonathan Outin, Michel Ondarts, Hugo Lange, Laurence Bois, Nolwenn Le Pierrès

Comparative experiments on a novel $CaCl_2$-based composite material and zeolite 13X inside a sorption reactor for solar heat storage

Elise Bérut[1], Jonathan Outin[1], Michel Ondarts[1], Hugo Lange[1], Laurence Bois[2] and Nolwenn Le Pierrès[1]

[1] Université Savoie Mont-Blanc, CNRS, LOCIE UMR 5271, F-73370 Le Bourget-du-Lac (France)

[2] Université Claude Bernard Lyon 1, CNRS, LMI UMR 5615, F-69622 Villeurbanne (France)

Abstract

A novel sorbent material made of a silica matrix, polymer PEG-600 and 34% by weight of salt hydrate $CaCl_2$ was experimentally studied for thermochemical heat storage applications and compared to zeolite 13X, which is a commonly used material in this field. Four desorption / sorption cycles were carried out using 56 g of composite sorbent in a fixed bed reactor and a dry air flow rate of about 0.14 normal liter s^{-1}. The desorption temperature was set at 130 °C, while sorption was conducted with an air flow at 30 °C and 42% relative humidity. The resulting water sorption capacity is 0.37 g g^{-1} of dehydrated material, that is twice that obtained with zeolite 13X BFK in the same conditions. The energy density is also improved by 60% compared to zeolite: on average, its value was evaluated to be 782 kJ kg^{-1} of dehydrated material. Lastly, the sorption kinetics is much slower when using the salt composite. Saturation ($P_{v,out}/P_{v,in} = 0.95$) is reached after about 12 h, instead of 2 h 30 with zeolite.

Keywords: thermochemical storage, water sorption, composite, calcium chloride, silica

1. Introduction

Energy generation from renewable sources such as wind or solar radiation supports infrastructure resilience and reduces vulnerability to climate change (IPCC, 2022). Renewable energies are clean, abundant and decentralized, but they are also intermittent in nature, thus requiring energy storage systems. These systems allow for meeting variable energy demands despite the inability to produce renewable energy for 24 h a day. Heat storage technologies can also be used for waste heat recovery in many areas such as building, textile, automobile, health care, agriculture or food processing, thereby increasing energy efficiency on a large scale.

Since energy is mostly used for heating and cooling applications (Connolly *et al.*, 2014; European Commission, 2016), thermal energy storage has been extensively investigated. It includes sensible, latent and thermochemical heat storage. The latter is particularly attractive because heat is stored as chemical potential energy, which prevents heat loss during long-term storage. Besides, thermochemical energy storage (TCES) systems are able to achieve high energy densities (Desai *et al.*, 2021). However, they are still in the early stage of the development process. TCES systems are based on reversible sorption phenomena involving chemical or physical bonding: the phenomena for charging and discharging heat are endothermic and exothermic, respectively.

In the present experimental work, the TCES setup is at the laboratory scale and based on water vapor sorption, whose principle is presented in eq. 1 (Mette *et al.*, 2014):

$$A_{(s)} + n.H_2O_{(g)} \rightleftarrows A.n.H_2O_{(s)} + \Delta H_s \qquad \text{(eq. 1)}$$

The TCES system is discharged by bringing the solid sorbant A in contact with water vapor, which bonds chemically or physically with the reactant. The solid product $A.n.H_2O$ is thus formed and the heat of sorption ΔH_s is released. During the charging process, also called desorption, the heat ΔH_s is supplied to the material, which is again dissociated into sorbent A and sorbate H_2O.

Open TCES systems based on water vapor sorption can be coupled to solar thermal collectors such as flat plate or evacuated tube collectors, as depicted in Fig. 1. During sunny days, the sorbent is dehydrated using a dry air stream heated to more than 80 °C by the solar collectors. In this work, evacuated tube solar collectors are assumed to reach at least 130 °C during the charging phase. The sorbed water is extracted from the sorbent bed by the air stream, which becomes wetter and cooler and is eventually rejected outside. Since this process is endothermic, it allows heat storage. During cold periods, the stored heat can be released through hydration of the sorbent. To this end, a humid air stream is sent from the building into the sorbent bed. Part of the water vapor is then sorbed by the material. Since the sorption is exothermic, a dry and hot air stream exits the bed, which can be used for domestic space heating if its temperature is above 30 or 35 °C. This air stream cannot however be blown directly into the heated space because it has been in contact with the sorbent: a heat exchanger must be included (Fig. 1) to comply with safety requirements. The heat exchanger can also be used to reduce the overall energy consumption of the process (Tatsidjodoung *et al.*, 2016): during sunny days, it allows recovering the remaining heat of the air stream exiting the sorbent bed to pre-heat the ambient air entering the solar collectors. Lastly, during the coldest periods and depending on the size and performance of the sorbent bed, an auxiliary heater may be called for in order to meet the heating demand.

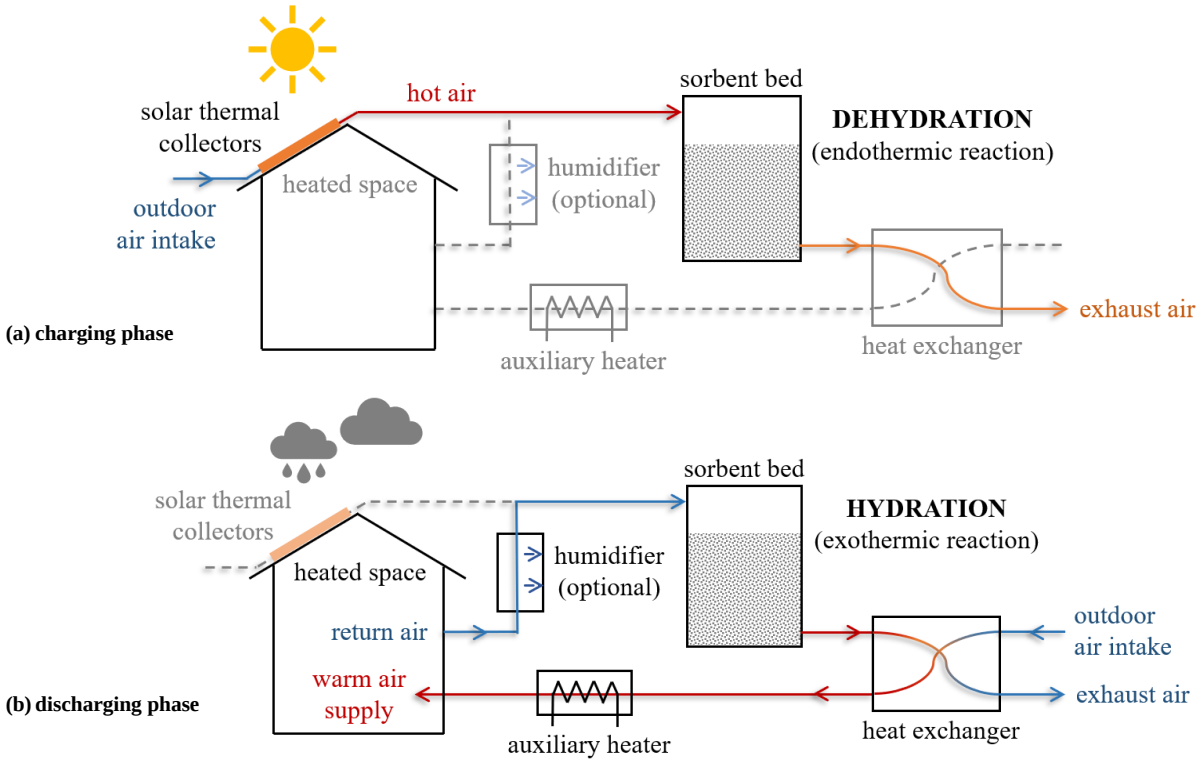

Fig. 1: Operating principle of an open TCES system based on water sorption coupled with solar thermal collectors

The viability of TCES systems depends on many parameters, not least the energy density of the storage material. Developing high energy density materials is essential for the systems to be compact and thus suitable for a wide range of applications, especially in the residential sector or vehicle industry. The most promising materials in this regard are salt hydrates, but their performance under actual operating conditions is unsatisfactory, mainly because of agglomeration, melting or deliquescence leading to poor heat and mass transfer (Zhao *et al.*, 2021). Consequently, composite materials are developed by impregnating salts into the pore structure of a host matrix, which exhibits a high specific surface area. The matrix promotes water-salt sorption interactions and is able to hold the salt and its solutions within its internal pore system (Lin *et al.*, 2021; Zhao *et al.*, 2021).

A novel composite material for TCES is studied in this paper. It is composed of a silica matrix, polymer PEG-600 and salt $CaCl_2$. This hydrophilic salt was chosen because it is able to react with water molecules at suitable temperature for the system (Fig. 1). Besides, composite materials containing calcium chloride exhibit the highest storage capacities and seem to be the most promising candidates among the different salt composites used for thermal storage applications (Jabbari-Hichri *et al.*, 2017; Lin *et al.*, 2021; Touloumet *et al.*, 2021; Xie *et al.*, 2019). The experimental storage performance of the composite material is compared with that obtained using zeolite 13X, which is a well-known sorbent material for this application.

2. Experimental heat storage setup

2.1. Description of the test facility

An open-cycle sorption storage system was designed (Fig. 2). It consists of a 46 mm inner diameter fixed bed reactor, a direct contact bubbling humidifier and a heating apparatus. The entering air flow rate is controlled by a mass flow controller. The uncertainty in this flow rate has been estimated to 0.004 normal liter s^{-1} over the range 0.03 to 0.30 normal liter s^{-1}. During the sorption phase, entering air is first saturated with water at a given temperature by flowing through the bubbler humidifier and then heated in order to reach the desired conditions (temperature and humidity) at the entrance of the reactor. The humidification temperature is controlled with a thermostatic bath. During charging (desorption), on the other hand, the humidifier is by-passed so that hot dry air enters the reactor.

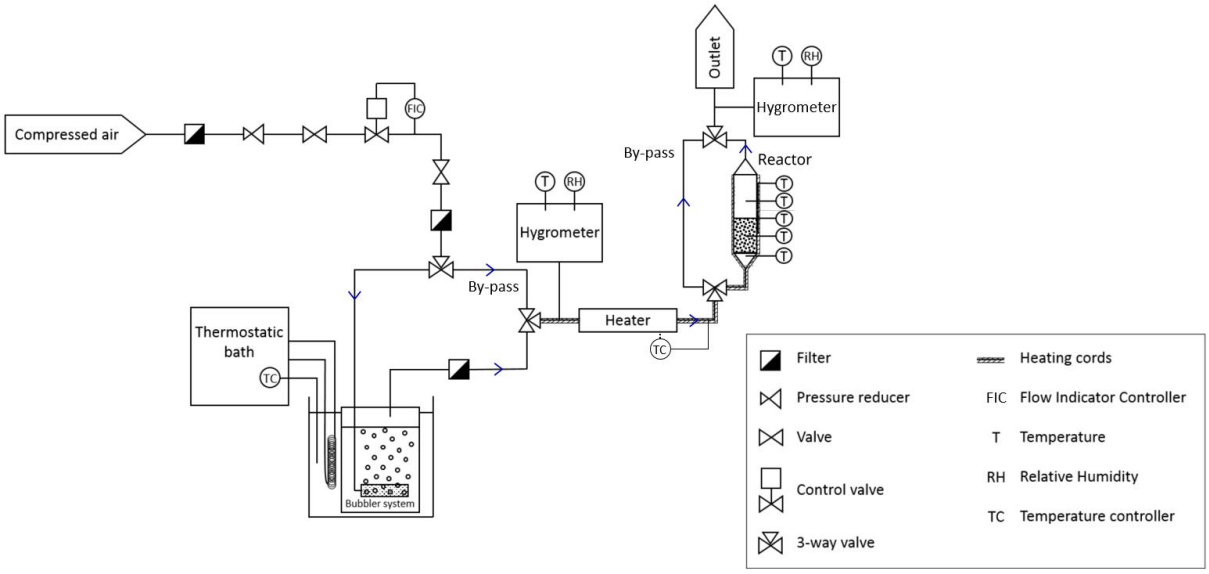

Fig. 2: Schematic of the experimental setup for the study of water sorption on a novel composite material

The air temperature and relative humidity at the inlet and outlet of the reactor are monitored using chilled mirror hygrometers (GE Sensing Optisonde D2). K-type thermocouples are placed inside the reactor, which is thermally insulated. Before testing, they have been calibrated over a 5 °C to 85 °C temperature range. The resulting uncertainty in temperature measurements is ± 0.5 °C. The location of the thermocouples is shown in Fig. 3. They are numbered from T_1 (bottom, reactor inlet) to T_5 (top, reactor outlet). Only one thermocouple is located inside the sorbent bed because of the limited amount of synthetized sorbent material. During experiments, measurements are recorded every ten seconds using LabVIEW acquisition software.

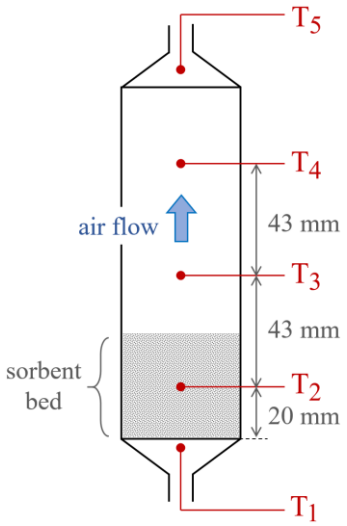

Fig. 3: Location of thermocouples T_1 to T_5 along the reactor

2.2. Testing procedure

Nominal experiments were conducted using 56 g of sorbent material and a dry air flow rate of about 0.14 normal liter s^{-1}, which leads to an acceptable pressure drop across the reactor. This flow rate leads to a bulk velocity of about 0.1 m s^{-1} through the sorbent bed, which falls within the usual range for sorption processes. The material, thereafter referred to as 'SC' for salt composite, was obtained by a sol-gel process. It contains 34% by weight of salt $CaCl_2$, as well as silica and polymer PEG-600. This salt content is close to that reported in previous studies about silica-$CaCl_2$ composites (Courbon *et al.*, 2017; Dawoud and Aristov, 2003; Jänchen *et al.*, 2004; Levitskij *et al.*, 1996; Touloumet *et al.*, 2021; Tso and Chao, 2012; Zheng *et al.*, 2014; Zhu *et al.*, 2006).

Prior to sorption, the sample is dried at 130 °C inside the reactor in order to remove residual moisture. Sorption is then performed with an air flow at 30 °C at the entrance of the reactor (temperature T_1) and 42% RH. These conditions are close to those found in residential buildings. To regenerate the sample, dry air at 130 °C is blown into the reactor during 4 h. This desorption temperature was set according to the outlet temperatures achievable by solar air collectors (Vengadesan and Senthil, 2020). Next, heating is switched off for the system to cool down. A new sorption cycle is then carried out and so on. Four successive desorption / sorption cycles were completed. A similar set of experiments was conducted using zeolite 13X BFK (Köstrolith® supplied by CWK, beads diameter from 1.2 to 2.0 mm). Three cycles were realized in this case in order to compare the results with those obtained with SC. The sorbent bed is slightly thinner when using zeolite instead of SC because it is more compact (bulk density increased by 13%). Still, the bed thickness is close to 40 mm in both cases.

2.3 Measurement data processing

The amount of water sorbed during each cycle is evaluated through a mass balance on the water vapor contained in the air flow. The mass balance is integrated over the duration of the sorption phase, yielding the following equation:

$$m_w = \int \dot{m}_w \, dt = \int \dot{m}_{da}(x_i - x_o)dt \approx \dot{m}_{da} \sum (x_i - x_o)\Delta t \qquad \text{(eq. 2)}$$

where $\dot{m}_w$ is the instantaneous mass flow rate of water sorbed by the material, $\dot{m}_{da}$ is the constant dry air flow rate going through the reactor, x_i and x_o are the specific humidities at the reactor inlet and outlet (in grams of water vapor per gram of dry air) and Δt is the time interval between two measurement readings.

Similarly, the sensible heat given to the air flow during the sorption phase is calculated as follows:

$$Q_{air} = \int \dot{Q}_{air} \, dt = \int \dot{m}_{da} \, c_{p,ha}(T_4 - T_1)dt \approx \dot{m}_{da} \sum c_{p,ha}(T_4 - T_1)\Delta t \qquad \text{(eq. 3)}$$

The heat capacity $c_{p,ha}$ of the *outlet* humid air is used in order to assess the potential for heat recovery by means of a heat exchanger placed after the reactor as closely as possible. In addition, the temperature T_4 is considered in the energy balance instead of T_5 to minimize the impact of thermal losses, and instead of T_3 for better temperature homogeneity over the channel cross-section.

The required properties of humid air (relative and specific humidity, specific heat capacity, water vapor partial pressure) are calculated using the CoolProp library (Bell *et al.*, 2014) from the dry bulb and dew point temperatures provided by each hygrometer.

Subsequently, the amount of sorbed water and the generated heat are expressed by mass or by volume of dehydrated material (at 130 °C for 4 h). The bulk density of dry SC was estimated to be 710 ± 70 kg m^{-3}, while that of zeolite is 800 ± 100 kg m^{-3}.

The heat loss from the reactor can be evaluated using the following relation:

$$Q_{loss} = U \int (\bar{T}_i - T_{amb})dt \approx U \sum (\bar{T}_i - T_{amb})\Delta t \qquad \text{(eq. 4)}$$

The overall heat transfer coefficient U between the ambient and the isolated reactor was determined experimentally in steady state using an inert material. It is about 0.0285 W K^{-1}. The heat loss also depends on the difference between $\bar{T}_i$, which is the mean temperature between T_1, T_2, T_3 and T_4, and the ambient temperature T_{amb} at each time step.

Finally, knowing the heat loss, the enthalpy of sorption of the material ΔH_s can be estimated under the tested conditions (humid air at 30 °C and 42% RH). Since the total energy stored in the reactor wall is negligible during

the sorption phase, it can be expressed as:

$$\Delta H_s = (Q_{air} + Q_{loss})/m_w \quad \text{(eq. 5)}$$

The enthalpy of sorption obtained in J g_{H2O}^{-1} can be compared to that measured by thermogravimetric analysis at the milligram scale.

2.4 Thermogravimetric analysis (TGA)

The enthalpy of sorption of the composite material was measured using a thermogravimetric analyzer coupled to a differential scanning calorimeter (Mettler Toledo, TGA/DSC 3+) and to a humidity generator (ProUmid MHG). The sample, which weights about 20 mg, is placed in an open alumina cell. It is first dehydrated under dry air flow at 30 °C for 24 h. Then, hydration is performed during 120 h under humid air flow at 30 °C and 42% RH, i.e., in the same conditions as those fixed at the reactor inlet during the sorption phase. The hydration step resulted in an exothermic peak on the heat flow curve. The integration of this signal enables the determination of the generated heat and, when expressed by mass of sorbed water, of the enthalpy of sorption. The relative error on the final value is about 5%.

3. Experimental heat storage results

3.1 Sorption kinetics

The breakthrough curves are presented in Fig. 4 for the four cycles carried out with SC. Such curves are used to characterize the sorption kinetics and to evaluate the sorption capacity of the tested material. Here, they are obtained from the ratio of the water outlet partial pressure $P_{v,out}$ to the water inlet partial pressure $P_{v,in}$.

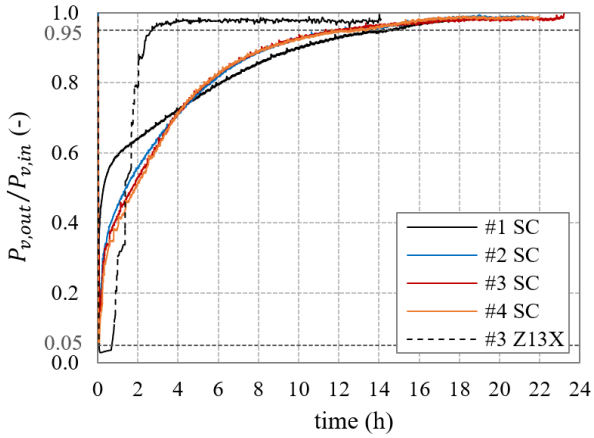

Fig. 4: Breakthrough curves during water sorption using SC and zeolite

The shape of the curve is significantly altered between the first cycle (black solid line) and second cycle (blue line). This is likely due to a change in the initial properties of the material. After that, curves #2 to #4 are overlapping, showing that the cycles are nearly identical and that SC properties are virtually stable. Fig. 4 also includes the breakthrough curve obtained with a similar mass of zeolite 13X (dashed line). Three cycles were performed in this case but, since all the curves overlapped, only that of the last cycle is presented to improve readability. Breakthrough takes place when the sorbate (water) starts to be detected at the outlet of the reactor. In this work, the breakthrough time has been taken when the vapor outlet partial pressure reaches 5% of the vapor inlet pressure ($P_{v,out}/P_{v,in} = 0.05$). Thus, breakthrough occurs after about 40 minutes with zeolite, while it is immediate for SC, which never fully sorbs the water vapor provided at the inlet for the considered bed thickness. Further, when using zeolite, the curve has a greater slope and saturation is reached much faster. Indeed, around 2 h 30 are required to reach saturation ($P_{v,out}/P_{v,in} = 0.95$) with zeolite, compared to 12 h for SC. The sorption kinetics of SC is thus much slower than that of zeolite. It may be limited by chemical kinetics, heat transfer or by water mass diffusion across the sorbent bed. The slow sorption kinetics of SC can be an advantage or a drawback depending on the considered application and the required power level.

The evolution of temperatures T_1 to T_5 during the sorption phase is shown in Fig. 5 for SC and zeolite. The temperature level is lower when using SC than zeolite. The maximum temperature is indeed around 54 °C in the

former case and 81 °C in the latter. This difference can be explained by the much slower sorption kinetics of SC. The temperatures return to their initial value (30 °C) after more than 10 h for SC versus 4 h for zeolite.

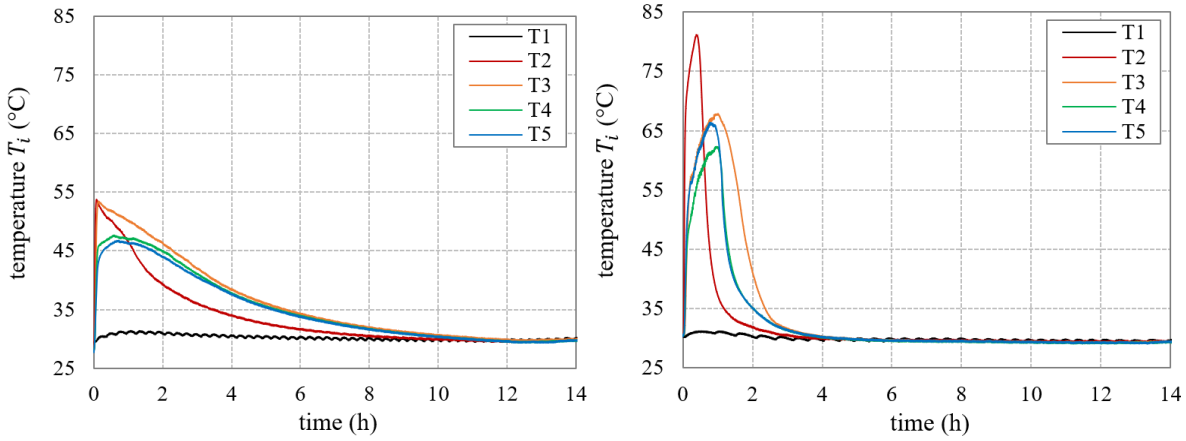

Fig. 5: Temperature curves over the sorption phase using SC (left, cycle #4) and zeolite (right, cycle #3)

3.2 Comparative performance analysis

The water sorption capacity of both sorbents (eq. 2) is given in Table 1, as well as the generated energy (eq. 3) and power during the sorption process for each cycle. The uncertainty in each value is indicated following a plus or minus sign. Uncertainties are evaluated using error propagation formulas and include the precision of the measuring instruments, the reproducibility of measurements and the uncertainties due to calibrations. Table 1 shows that the sorption capacity of SC is on average twice that of zeolite. As a result, the generated energy and the mass energy density increase by nearly 60% when SC is used instead of zeolite. The mass energy density amounts on average to 782 kJ kg^{-1} of dehydrated material for SC and to 493 kJ kg^{-1} for zeolite. The fact that the energy is not doubled can be partly explained by a weaker binding energy between water vapor molecules and SC sorbent than between water and zeolite (see part 3.4). The volumetric energy density increases slightly less than the mass energy density (+ 40%) because SC is less compact than zeolite. Finally, the maximum power is two times lower with SC, which is consistent with the temperature curves of Fig. 5.

Tab. 1: Comparison of water sorption capacity, generated energy and power (sensible heat) with SC and zeolite

	SC				**Zeolite 13X BFK**		
cycle	#1	#2	#3	#4	#1	#2	#3
quantity of sorbed water m_w (g)	20.3 ± 2.8	20.9 ± 2.9	21.3 ± 3.2	21.9 ± 3.1	10.7 ± 2.3	9.7 ± 2.2	11.6 ± 2.3
water sorption capacity (g_{H2O} g^{-1})	0.36 ± 0.06	0.37 ± 0.06	0.38 ± 0.07	0.39 ± 0.07	0.19 ± 0.05	0.17 ± 0.05	0.21 ± 0.05
generated energy Q_{air} (kJ)	37.4 ± 1.9	44.9 ± 2.3	48.1 ± 2.5	45.6 ± 2.3	26.3 ± 1.4	29.7 ± 1.6	27.1 ± 1.4
energy density (kJ kg^{-1})	665 ± 59	798 ± 70	856 ± 76	811 ± 71	468 ± 36	528 ± 41	482 ± 36
energy density (kWh m^{-3})	131 ± 18	157 ± 21	169 ± 23	160 ± 22	104 ± 16	117 ± 18	107 ± 16
maximum power $\dot{Q}_{air,max}$ (W)	1.7 ± 0.3	2.9 ± 0.3	3.1 ± 0.3	3.1 ± 0.3	5.6 ± 0.5	5.9 ± 0.6	5.8 ± 0.5

The energy densities estimated for zeolite are consistent with literature values. Jänchen *et al.* (2012) found a storage density of 600 kJ kg^{-1} for the binderless zeolite 13X they have synthetized and tested in an open storage apparatus (desorption at 200 °C, sorption at 23 °C and 35% RH). Bennici *et al.* (2020) studied the same zeolite that we used and give an energy density of about 850 kJ kg^{-1}. It was measured through TGA during hydration with an air flow at 30 °C and 60% RH. This high relative humidity partly explains the greater energy density found by the authors. The discrepancy is also due to the fact that the heat loss from the reactor was neglected in Table 1. As a result, the generated energies and powers are systematically underestimated in the present analysis. Two studies characterized the storage performance of zeolite 13X at a larger scale: Bales *et al.* (2008) obtained an energy density of 180 kWh m^{-3} and a maximum power of 800 W from a storage reactor containing 7 kg of zeolite, while Hauer (2007) found an energy density of 124 kWh m^{-3} and a maximum power of 130 kW for a scaled-up system containing 7 000 kg of zeolite.

To return to the composite material, the evolution of the results over the four cycles is worth examining. The quantity of water sorbed by SC is marginally altered from cycle #1 to cycle #4. The generated energy and power, however, increase significantly (+ 20% and + 70%) between the first and second cycles. Then, they are more stable, with a maximum variation of 7% between cycles. These results are consistent with the modification of the sorption kinetics observed in Fig. 4 between the first cycle and the next ones. According to Fig. 4, the quantity of water sorbed during the first four hours of cycle #1 is reduced compared to that sorbed at the beginning of the next cycles, which notably explains the variation of the maximum power shown in Table 1.

3.3 Hydration states of $CaCl_2$

Several salt hydrates have been identified and should theoretically appear successively during water sorption on calcium chloride at 30 °C: $CaCl_2{\cdot}H_2O$, $CaCl_2{\cdot}2H_2O$, $CaCl_2{\cdot}4H_2O$ and $CaCl_2{\cdot}6H_2O$ (Aristov, 2020). Then, above 1 gram of sorbed water per gram of salt, the latter dissolves and reaches the liquid state. In this study, the salt sorbs on average 1.10 g_{H2O} g^{-1} (or 6.8 mol_{H2O} mol^{-1} of $CaCl_2$), so part of it has likely turned to liquid inside the matrix pores. However, according to Aristov (2020), the properties of a confined salt differ from that of a bulk one. The transitions between hydration states may thus be modified depending on the composite structure.

Under the chosen experimental conditions, Table 1 shows that the quantity of water sorbed by SC is slightly increasing from one cycle to the next, and there is no performance degradation indicative of salt leakage. The host matrix thus managed to stabilize the hydrated calcium chloride. Still, special attention must be paid to salt leakage because $CaCl_2$ solutions are highly corrosive and the risk of leakage increases when operating at high humidities. A thorough characterization of the material is required to ensure its stability under a wide range of operating conditions.

3.4 Enthalpy of sorption

The enthalpy of sorption is the heat released by the sorption of a given amount of water. It characterizes the bonding strength between the water vapor molecules and the sorbent. It was measured both by TGA (see section 2.4) and at the reactor scale using eq. 5 (which includes the heat loss). The results obtained with SC are summarized in Table 2.

Tab. 2: Enthalpy of sorption of SC measured by TGA and estimated using eq. 5

cycle	#1	#2	#3	#4
ΔH_s measured by TGA (J g_{H2O}^{-1})		3275		
ΔH_s measured at the reactor scale (J g_{H2O}^{-1})	2450	2720	2830	2630
difference (%)	- 25	- 17	- 14	- 20

The uncertainty in the values from eq. 5 is significant (± 25%) because they depend on the heat loss, which is estimated. Besides, the mass of the sample analyzed by TGA amounts to a few tens of milligrams. Material inhomogeneities could therefore have a strong impact on the result. Despite these potential sources of error, the order of magnitude of the enthalpies are consistent between both methods, with a maximum deviation of 25%.

The enthalpy of sorption of the tested zeolite was evaluated by TGA to be 3450 J g_{H2O}^{-1} (Polimann, 2019). The analysis was however performed under conditions distinct from those of our experiments (25 °C, unspecified humidity). Still, the values calculated at the reactor scale from eq. 5 are comparable: on average, the enthalpy of sorption of zeolite is estimated to be 2980 J g_{H2O}^{-1} (- 14% compared to the TGA value).

Finally, the energy released during the sorption of a given mass of water is more important with zeolite than with SC: on average, the estimated enthalpy of sorption in J g_{H2O}^{-1} decreases by 11% with the latter. Yet, physical bonds are created in the first case (physisorption), while high-energy chemical bonds are supposed to form in the second case (chemisorption during hydration of $CaCl_2$). This apparent contradiction could be explained by the physisorption of part of the water on the silica matrix of the composite, thus decreasing the mean energy released. A control material containing only silica and PEG will be tested in the near future in order to quantify the actual benefit of adding calcium chloride. Regardless, the energy density of SC remains higher than that of zeolite due to its high sorption capacity.

4. Conclusion

Thermochemical heat storage is a promising technology to support the development of renewable energy on a large scale. The heat storage performance of a new composite material obtained by a sol-gel process has been characterized in an open-cycle sorption reactor, with moist air as the sorbate and heat transfer fluid. The salt composite (SC) contains 34% by weight of anhydrous calcium chloride ($CaCl_2$) dispersed in a matrix of silica and polymer PEG-600. Similar experiments were conducted using zeolite 13X BFK for comparison.

The average sorption capacity of SC is 0.37 grams of water per gram of dehydrated material, which is twice that of zeolite. The energy generated during the sorption of a given mass of water is however slightly increased when using zeolite. Indeed, the enthalpy of sorption measured by TGA (and consistent with that obtained at the reactor scale) is 3275 J g_{H2O}^{-1} for SC, compared to about 3450 J g_{H2O}^{-1} for zeolite. Thanks to its high sorption capacity, the energy density of SC is still increased by nearly 60% compared to that of zeolite (782 kJ kg^{-1} on average, versus 493 kJ kg^{-1} for zeolite).

The sorption kinetics is much slower when using SC than zeolite: around 12 h are required for SC to reach water vapor saturation ($P_{v,out}/P_{v,in} = 0.95$), compared to 2 h 30 with zeolite. Besides, breakthrough occurs immediately in the first case, and after 40 minutes in the second case. The slow sorption kinetics of SC leads to reduced temperatures and generated powers during the sorption phase. The maximum power is indeed two times smaller with SC than with zeolite. The temperatures are still around 50 °C, which is adequate for space heating applications.

The host matrix managed to stabilize the hydrated calcium chloride and to avoid leakage under the chosen experimental conditions. However, operating at higher humidities could promote deliquescence. A thorough characterization of the material is thus needed to ensure its stability under a wide range of operating conditions. The influence of the salt content on the risk of leakage and on the storage performance is also worth investigating.

Acknowledgments

This work was supported by the French National Research Agency (ANR) in the frame of the STOCK-CAR project, which is carried out in collaboration with IRCELYON (Institut de Recherche sur la Catalyse et l'Environnement de Lyon, UMR 5256), LMCPA (Laboratoire des Matériaux Céramiques et Procédés Associés, EA 2443) and LMI (Laboratoire des Multimatériaux et Interfaces, UMR 5615).

References

Aristov, Y.I., 2020. Nanocomposite sorbents for multiple applications. Jenny Stanford Publishing: Singapore, 446 p., ISBN 9789814267502.

Bales, C., Gantenbein, P., Jaenig, D., Kerskes, H., Summer, K., van Essen, M., Weber, R., 2008. Laboratory tests of chemical reactions and prototype sorption storage units. A report of IEA Solar Heating and Cooling programme, Task 32 – Report B4 of Subtask B.

Bell, I.H., Wronski, J., Quoilin, S., Lemort, V., 2014. Pure and pseudo-pure fluid thermophysical property evaluation and the open-source thermophysical property library CoolProp. Industrial & Engineering Chemistry Research, 53, 2498-2508.

Bennici, S., Polimann, T., Ondarts, M., Gonze, E., Vaulot, C., Le Pierrès, N., 2020. Long-term impact of air pollutants on thermochemical heat storage materials. Renewable and Sustainable Energy Reviews, 117, 109473.

Connolly, D., Lund, H., Mathiesen, B.V., Werner, S., Möller, B., Persson, U., Boermans, T., Trier, D., Østergaard, P.A., Nielsen, S., 2014. Heat Roadmap Europe: combining district heating with heat savings to decarbonise the EU energy system. Energy Policy, 65, 475-489.

Courbon, E., D'Ans, P., Permyakova, A., Skrylnyk, O., Steunou, N., Degrez, M., Frère, M., 2017. Further improvement of the synthesis of silica gel and $CaCl_2$ composites: Enhancement of energy storage density and stability over cycles for solar heat storage coupled with space heating applications. Solar Energy, 157, 532-541.

Dawoud, B., Aristov, Y., 2003. Experimental study on the kinetics of water vapor sorption on selective water sorbents, silica gel and alumina under typical operating conditions of sorption heat pumps. International Journal of Heat and Mass Transfer, 46, 273-281.

Desai, F., Prasad, J.S., Muthukumar, P., Rahman, M.M., 2021. Thermochemical energy storage system for cooling and process heating applications: A review. Energy Conversion and Management, 229, 113617.

European Commission, 2016. Communication from the Commission to the European Parliament, the Council, the European Economic and Social Committee and the Committee of the Regions - an EU Strategy on Heating and Cooling. Brussels, COM/2016/051 final.

Hauer, A., 2007. Adsorption systems for TES – Design and demonstration projects. Proceedings of the Thermal Energy Storage for Sustainable Energy Consumption Conference, Dordrecht, 409-427.

IPCC, 2022. Climate change 2022: impacts, adaptation and vulnerability. Contribution of working group II to the sixth assessment report of the Intergovernmental Panel on Climate Change.

Jabbari-Hichri, A., Bennici, S., Auroux, A., 2017. $CaCl_2$-containing composites as thermochemical heat storage materials. Solar Energy Materials and Solar Cells, 172, 177-185.

Jänchen, J., Ackermann, D., Stach, H., Brosicke, W., 2004. Studies of the water adsorption on zeolites and modified mesoporous materials for seasonal storage of solar heat. Solar Energy, 76, 339-344.

Jänchen, J., Schumann, K., Thrun, E., Brandt, A., Unger, B., Hellwig, U., 2012. Preparation, hydrothermal stability and thermal adsorption storage properties of binderless zeolite beads. International Journal of Low-Carbon Technologies, 7, 275-279.

Levitskij, E.A., Aristov, Y.I., Tokarev, M.M., Parmon, V.N., 1996. "Chemical heat accumulators": a new approach to accumulating low potential heat. Solar Energy Materials and Solar Cells, 44, 219-235.

Lin, J., Zhao, Q., Huang, H., Mao, H., Liu, Y., Xiao, Y., 2021. Applications of low-temperature thermochemical energy storage systems for salt hydrates based on material classification: a review. Solar Energy, 214, 149-178.

Mette, B., Kerskes, H., Drück, H., Müller-Steinhagen, H., 2014. Experimental and numerical investigations on the water vapor adsorption isotherms and kinetics of binderless zeolite 13X. International Journal of Heat and Mass Transfer, 71, 555–561.

Polimann, T., 2019. Impact des polluants de l'air sur la durabilité de matériaux dédiés au stockage thermochimique de la chaleur solaire pour le bâtiment. *Ph.D. thesis*, Université Grenoble Alpes, France.

Tatsidjodoung, P., Le Pierrès, N., Heintz, J., Lagre, D., Luo, L., Durier, F., 2016. Experimental and numerical investigations of a zeolite 13X / water reactor for solar heat storage in buildings. Energy Conversion and Management, 108, 488-500.

Touloumet, Q., Silvester, L., Bois, L., Postole, G., Auroux, A, 2021. Water sorption and heat storage in $CaCl_2$ impregnated aluminium fumarate MOFs. Solar Energy Materials and Solar Cells, 231, 111332.

Tso, C.Y., Chao, C.Y.H., 2012. Activated carbon, silica-gel and calcium chloride composite adsorbents for energy efficient solar adsorption cooling and dehumidification systems. International Journal of Refrigeration, 35, 1626-1638.

Vengadesan, E., Senthil, R., 2020. A review on recent developments in thermal performance enhancement methods of flat plate solar air collector. Renewable and Sustainable Energy Reviews, 134, 110315.

Xie, N., Niu, J., Wu, T., Gao, X., Fang, Y., Zhang, Z., 2019. Fabrication and characterization of $CaCl_2 \cdot 6H_2O$ composite phase change material in the presence of Cs_xWO_3 nanoparticles. Solar Energy Materials and Solar Cells, 200, 110034.

Zhao, Q., Lin, J., Huang, H., Wu, Q., Shen, Y., Xiao, Y, 2021. Optimization of thermochemical energy storage systems based on hydrated salts: A review. Energy and Buildings, 244, 111035.

Zheng, S., Ge, T.S., Wang, R. Z., Hu, L.M., 2014. Performance study of composite silica gels with different pore sizes and different impregnating hygroscopic salts. Chemical Engineering Science, 120, 1-9.

Zhu, D., Wu, H., Wang, S., 2006. Experimental study on composite silica gel supported $CaCl_2$ sorbent for low grade heat storage. International Journal of Thermal Sciences, 45, 804-813.

Nomenclature

c_p	specific heat capacity at constant pressure, J K^{-1} g_{da}^{-1}
ΔH_s	enthalpy (or heat) of sorption, J g_{H2O}^{-1}
m	mass, g
$\dot{m}$	mass flow rate, g s^{-1}
P_v	water vapor partial pressure, Pa
Q_{air}	sensible heat given to the air flow, J
$\dot{Q}_{air}$	heat transfer rate, W
Q_{loss}	heat loss, J
t	time, s
T_{amb}	ambient temperature, °C
T_i	i^{th} temperature measurement along the reactor, °C
$\bar{T}_i$	average of temperatures T_1 to T_4, °C
U	overall heat transfer coefficient between the ambient and the reactor, W K^{-1}
x	specific humidity, g_{H2O} g_{da}^{-1}

Subscripts

da	dry air
ha	humid air
i	reactor inlet
max	maximum
o	reactor outlet
w	sorbed water

Acronyms

PEG	polyethylene glycol
RH	relative humidity
SC	salt composite
TGA	thermogravimetric analysis